HHS Public Access

Author manuscript

*Comp Biochem Physiol Part D Genomics Proteomics*. Author manuscript; available in PMC 2017 September 01.

Published in final edited form as:

*Comp Biochem Physiol Part D Genomics Proteomics*. 2016 September ; 19: 159–173. doi:10.1016/j.cbd.2016.04.003.

# Differential recruitment of co-regulatory proteins to the human estrogen receptor 1 in response to xenoestrogens☆,☆☆

**L. Cody Smith**[#a], **Jessica C. Clark**[#b], **Joseph H. Bisesi Jr**[#c], **P. Lee Ferguson**[#b], and **Tara Sabo-Attwood**[#c,*]

[a] Department of Physiological Sciences and Center for Environmental and Human Toxicology, University of Florida, Gainesville, FL 32611, USA

[b] Department of Civil and Environmental Engineering and Nicholas School of the Environment, Duke University, Durham, NC 27708, USA

[c] Department of Environmental and Global Health and Center for Environmental and Human Toxicology, University of Florida, Gainesville, FL 32611, USA

[#] These authors contributed equally to this work.

## Abstract

The diverse biological effects of xenoestrogens may be explained by their ability to differentially recruit co-regulatory proteins to the estrogen receptor (ER). We employed high-throughput receptor affinity binding and co-regulatory protein recruitment screening assays based on fluorescence polarization and time resolved florescence resonance energy transfer (TR-FRET), respectively, to assess xenoestrogen-specific binding and co-regulatory protein recruitment to the ER. Then we used a functional proteomic assay based on co-immunoprecipitation of ER-bound proteins to isolate and identify intact co-regulatory proteins recruited to a ligand-activated ER. Through these approaches, we revealed differential binding affinity of bisphenol-A (BPA) and genistein (GEN) to the human ERα (ESR1) and ligand-dependent recruitment of SRC-1 and SRC-3 peptides. Recruitment profiles were variable for each ligand and in some cases were distinct compared to 17β-estradiol (E2). For example, E2 and GEN recruited both SRC-1 and -3 peptides whereas BPA recruited only SRC-1 peptides. Results of the functional proteomic assay showed differential recruitment between ligands where E2 recruited the greatest number of proteins followed by BPA then GEN. A number of proteins share previously identified relationships with ESR1 as determined by STRING analysis. Although there was limited overlap in proteins identified between treatments, all ligands recruited proteins involved in cell growth as determined by subnetwork enrichment analysis ($p < 0.05$). A comparative, *in silico* analysis revealed that fewer interactions exist between zebrafish (*Danio rerio*) esr1 and zebrafish orthologs of proteins identified in our functional proteomic analysis. Taken together these results identify

☆This work was supported by NIH grant number 1R21ES16617.

☆☆Disclosure statement: All authors have nothing to declare.

* Corresponding author at: Department of Environmental and Global Health and Center for Environmental and Human Toxicology, University of Florida, 2187 Mowry Rd, Gainesville, FL 32611, USA. sabo@phhp.ufl.edu (T. Sabo-Attwood).

Conflict of interest

The authors declare that there are no conflicts of interest.

recruitment of known and previously unknown co-regulatory proteins to ESR1 and highlight new methods to assay recruitment of low abundant and intact, endogenous co-regulatory proteins to ESR1 or other nuclear receptors, in both human and aquatic species.

**Keywords**

Estrogen; Estrogen receptor; Xenoestrogens; Fluorescence polarization; Time resolved fluorescence resonance energy transfer; Steroid receptor co-regulator, co-immunoprecipitation, proteomics

## 1. Introduction

Estrogen (E2) is a steroid hormone that controls a diverse array of normal biological processes in vertebrates but is also implicated in reproductive and non-reproductive disease (Dahlman-Wright et al., 2006). Classically, E2 exerts its effects through nuclear estrogen receptors (ERs), which are ligand-dependent transcription factors that regulate gene expression through a complex network of protein–protein and protein–DNA interactions (Gruber et al., 2002). Upon ligand induction, the ER undergoes a series of regulatory modulations, including dimerization, nuclear translocation, and recruitment of co-regulatory proteins to form a macromolecular transcriptional complex. This complex consists of co-activators and/or co-repressors that activate or repress downstream gene targets in response to agonists and antagonists, respectively (Gruber et al., 2002).

It has been hypothesized that differential association of the ERs with co-regulatory proteins directs activation at discrete promoter elements, leading to selectivity in downstream gene expression (Shibata et al., 1997; Shang and Brown, 2002). This phenomenon came to be known as the ‘co-activator hypothesis’ which describes how the same ligand can manifest different biological activities in discrete tissues within the same animal (McDonnell, 2005). For example, while TAM acts as an ER antagonist in human breast tissue, it acts as an ER agonist in other tissues (McDonnell et al., 2002). This further led to the realization that structurally diverse ER ligands could induce specific structural changes in the conformation of ERs, which lead to variations in co-regulator protein affinity for the receptor, thus, impacting downstream gene activation or repression. (McDonnell et al., 2002).

To date, over 30 ER co-regulatory proteins have been identified in mammalian systems which interact with ER transcriptional complex machinery in response to E2 and alternate ligands. The most well-characterized ER complex members are those that comprise the p160 family, including steroid receptor co-activators, SRC-1 (NCoA-1), SRC-2 (TIF2, GRIP-1), and SRC-3 (AIB1, ACTR, p/CIP, RAC3, TRAM-1) (Karmakar et al., 2009). SRC-1, has demonstrated direct binding of specific peptides to the ER in response to E2 through yeast two-hybrid and phage ELISA assays (Hall and Korach, 2002; Lee et al., 2002). Interactions between ER and SRCs have also been suggested in activation of the receptor by employing siRNA strategies as loss of SRC-1 or -3 alters E2-driven cellular processes in human astrocytoma cells (González-Arenas et al., 2012). The family of p160 proteins are also highly expressed in a number of tumors and have been proposed to account for resistance to therapeutics such as aromatase inhibitors or TAM (Tikkanen et al., 2000b; Lauritsen et al.,

2002; Xu and Li, 2003; Shao et al., 2004; Labhart et al., 2005; Karmakar et al., 2009; McBryan et al., 2012), highlighting their importance in disease development and treatment regimes.

While the interaction of co-accessory proteins with the ER in response to the endogenous ligand E2 has been rigorously examined, modulation by environmentally-relevant chemicals has yet to be explored in-depth. Hormonally active agents compose a diverse class of natural and synthetic compounds (Kuiper et al., 1998a; Sonnenschein and Soto, 1998; Okubo et al., 2004), and can disrupt steroid signaling in organisms through a variety of mechanisms. For example, xenoestrogens alter E2 signaling by modulation of endogenous steroid synthesis and/or direct modulation of the ERs through agonist or antagonistic means (Shanle and Xu, 2010). Many of these xenoestrogens have been causally linked to adverse health outcomes in target organisms when exposed under environmental conditions (Bergman et al., 2012).

Differential recruitment of co-regulatory proteins represents an additional plausible mechanism for endocrine disruption in humans and other species exposed to xenoestrogens. To date, research on the ligand-dependence of co-regulatory protein recruitment to ERs has focused primarily on therapeutic SERMs that have been used in recent years for the treatment of ER-positive breast cancers. These studies indicated that structurally diverse ligands can drive differential recruitment of co-regulatory proteins within a single cellular context. While most of the investigations of ER-co-regulatory recruitment have focused on the well-studied p160 family members (SRCs) in response to E2, only a handful of studies have reported interactions of these proteins with the receptor in response to binding of ER by the xenoestrogens genistein (GEN), diethylstilbestrol, (DES), bisphenol-A (BPA), and nonylphenol (NP). These targeted analyses were performed primarily by employing glutathione S-transferase (GST) pull-down, combinatorial phage display, yeast two hybrid, and surface plasmon resonance assays (Nishikawa et al., 1999; Paige et al., 1999; Kraichely et al., 2000; Parker et al., 2000; Routledge et al., 2000; Wong et al., 2001), although there is growing interest in employing non-targeted methods to evaluate global co-regulatory protein recruitment.

Based on the current gaps in knowledge, the objectives of our study were to investigate xenoestrogen-induced activation of the human estrogen receptor α (hERα, also known as ESR1) using a suite of *in vitro*, high-throughput real-time receptor binding (fluorescent polarization) assays, to investigate the potential for ligand-specific co-regulatory protein recruitment by SRC-1 and SRC-3 recruitment assays (time resolved fluorescent resonance energy transfer, TR-FRET), and to identify intact co-regulatory proteins bound to endogenous E2- and xenoestrogen-activated ESR1 transcriptional complexes using a co-immunoprecipitation method. Finally, we sought to take a comparative approach to both highlight the utility of our methods in the assessment of differential co-regulatory protein recruitment to nuclear receptors in aquatic species and to compare co-regulatory protein recruitment between human ESR1 and zebrafish (*Danio rerio*) esr1 in response to E2 binding as ER signaling pathways are moderately conserved across species (Lam et al., 2011).

## 2. Materials and methods

### 2.1. Mammalian cell culture

MCF-7 cells (American Type Culture Collection (ATCC), Manassas, VA) were cultured in phenol-red free Eagle's Minimum Essential Medium (MEM, Corning cellgro, 17305-CV) supplemented with 0.1 mM nonessential amino acids, 1 mM sodium pyruvate, 1% penicillin–streptomycin (Hyclone, SV30010), 1.5 g/L sodium bicarbonate (Corning cellgro, 25-035-CL), 1% L-glutamine (25-005-CI), and 10% fetal bovine serum (Corning cellgro, 35-010-CV). Human Embryonic Kidney 293 (HEK293) cells (ATCC) were cultured in phenol-red free Dulbecco's Modified Essential Medium (DMEM, Corning cellgro, 17-205-CV) supplemented with 1% L-glutamine, 1% penicillin–streptomycin, and 10% fetal bovine serum.

### 2.2. Fluorescence polarization ligand binding assay

Fluorescence polarization (FP) was first proposed by Adamczyk et al. (2002)) and offers significant advantages compared to conventional radioligand binding protocols. Unlike radioligand-based assays, the FP assay is performed in a homogeneous format that relies on displacement of a fluorescent-labeled estrogen probe from free-solution ER in order to calculate relative binding affinities of ligands. All ligands (17β-estradiol (E2, Sigma, 2578), 4-OH-tamoxifen (TAM, Sigma, T5648), Genistein (GEN, Sigma, G6649), and bisphenol-A (BPA, supplied by NIEHS)) were prepared as concentrated stocks in DMSO and further diluted into binding buffer (10 mM Tris–HCl pH 7.4 (Sigma, 154,563), 50 mM KCl (Sigma, P5405), 10% glycerol (Sigma, G5516), 0.1 mM DTT (Promega, V3151), 0.02% sodium azide (Sigma, S2002), 1 μg/mL bovine gamma globulin (BGG, Sigma, G5009), 0.2% CHAPS (Sigma, C9426)). The pET-32b vector (Millipore, 69016) containing human estrogen receptor alpha ligand binding domain (ESR1-LBD, a gift of Marc Ruff, L'Institut de génétique et de biologie moléculaire et cellulaire (IGBMC), Strasbourg, France), was expressed in origami cells (Millipore) and purified by HPLC (Agilent 1100). Serial dilutions of ligands were prepared in triplicate by adding 200 μL of the working ligand stocks to the first well of each row in a 96-well plate and transferring 100 μL to each additional well containing buffer. Purified ESR1-LBD was diluted and added to each well to give a final ER concentration of 10 nM. Finally, the fluorescent probe (F-$E_1$), an estrone conjugate coupled to fluorescein-5-thiosemicarbazide (FTSC), was added to give a final concentration of 0.5 nM. The plate was incubated at room temperature in the dark for 1 h prior to analysis. Fluorescence polarization (FP) was measured on a Biotek Synergy H1 spectrophotometer using an excitation wavelength of 485 nm and emission wavelength of 525 nm. FP was converted to percent inhibition ($I_{\%} = (A_0 - A) / (A_0 - A_{100}) * 100$) where A = absorbance and plotted against concentration of ligand using SigmaPlot 11 (Systat Software, Inc., San Jose, CA). Curves were fit by transforming the x-axis to a logarithmic scale and applying a nonlinear regression curve using a sigmoidal-dose response with variable slope to obtain $IC_{50}$ values for the corresponding ligands in SigmaPlot 11.

### 2.3. Time-resolved fluorescence resonance energy transfer (TR-FRET)

To elucidate the mechanism of xenoestrogen action in recruiting co-activators SRC-1 and SRC-3, we utilized a TR-FRET assay. In this assay, compounds were measured for their

ability to recruit model peptides derived from distinct adapter regions of the human SRC-1 and SRC-3 proteins to the ER-ligand complex. The peptides employed in the assay each contain an LXXLL motif and occur in the receptor interacting domain (RID) of the co-regulatory protein. One additional LXXLL peptide for SRC-1 is present in the C-terminal region of the protein (Fig. 2).The Lanthascreen estrogen receptor co-activator kit was purchased from Invitrogen Corporation (A15885), and each assay was performed following the manufacturer's instructions. Briefly, all compounds (E2, TAM, BPA, GEN) were serially diluted in DMSO to yield a 12-point dilution series (range of final concentrations 0.01 nM–10.0 μM). Aliquots (10 μL) of each ligand were transferred to 4 wells of a white low-volume 384-well plate (Corning Inc., Corning, NY). The ESR1 Ligand-binding domain tagged with glutathione-S-transferase (GST-ER LBD) was diluted to 4 × in complete buffer and 5 μL added to each well to give a final assay concentration of 7 nM. A premixed solution of 4 × fluorescein peptide and terbium labeled anti-GST antibody were diluted in complete buffer and 5 μL added to each well such that final assay concentrations were 250 nM and 5 nM, respectively. The assay plate was incubated for 1 h at ambient temperature in the dark followed by TR-FRET measurements in a Spectramax M5 dual monochromator spectrophotometer (Molecular Devices) with delay and integration times of 100 μs and 200 μs, respectively. The terbium species was excited at 340 nm with a bandwidth of 30 nm and both terbium and fluorescein emissions were measured at 478 and 520 nm, respectively. The emission ratio was calculated as the raw intensity of acceptor (520 nm) to donor (478 nm) fluorescence with 4 replicates measured per concentration of ligand. The dose–response curves were generated by plotting emission ratios (y axis) against ligand concentration (x axis) using Prism 4 (GraphPad Software, La Jolla, CA). The curves were analyzed by transforming the x-axis to a logarithmic scale and applying a nonlinear regression curve using a sigmoidal-dose response with variable slope using SigmaPlot 11 (Systat Software Inc., San Jose, CA).

### 2.4. Protein extraction

MCF-7 cells were cultured in phenol-red free Eagle's Minimum Essential Medium (MEM, Cellgro 17-305-CV, Manassas, VA) in T225 cell culture flasks. Exposures were conducted in triplicate for each compound (two flasks of confluent cells per replicate exposure, with an additional two flasks to serve as an IgG-only, non-specific binding control as described below) to 10 nM E2, 1 μM BPA, or 1 μM GEN, as well as to a DMSO carrier-control for a period of 3.5 h. Nuclear extracts were prepared with the Active Motif Nuclear Extract Kit (40,010). Briefly, media were aspirated from dishes and cells were washed with ice-cold PBS/phosphatase inhibitor solution. Cells were removed from each dish by gentle scraping and cells from individual plates for a given treatment replicate were pooled and washed with hypotonic buffer on ice. Lysis was performed with hypotonic lysis buffer by gentle pipetting. Lysates were centrifuged for 30 s at 14,000 × g at 4 °C and supernatant (cytosolic fraction) was discarded. Nuclear extracts were prepared from the pellet using a hypertonic digestion buffer with DNase using gentle vortexing. The extracts were clarified at 14,000 × g at 4 °C for 10 min and processed for immunoprecipitation immediately without freezing.

### 2.5. Co-immunoprecipitation of intact co-regulatory proteins

We applied a mass-spectrometry compatible immunoprecipitation (IP) strategy for isolating ER transcriptional complexes from nuclear extracts of xenoestrogen-exposed MCF-7 cells. In this method, anti-ESR1 antibodies (Active Motif, 61,035) were covalently crosslinked to protein A/G agarose (Pierce Biotechnology, 20,421) using dimethylpimelimidate (DMP, Pierce Biotechnology, 21,667) prior to immunoprecipitation of the complexes. For each IP reaction, 20–30 μg of antibody (either rabbit anti-ESR1 (Active Motif) or mouse IgG1 (Cell Signaling, 5415) for nonspecific-binding controls) were bound to 30 μL of protein A/G beads overnight in 1 mL PBS (Thermo Scientific, SH30256.01) prior to washing 3 × with 0.2 M sodium borate buffer (pH 9.0). Beads were resuspended in 1 mL of 0.2 M borate buffer containing 20 mM DMP and crosslinked for 40 min at room temperature. The crosslinked antibody beads (IgG and anti-ESR1) were washed 1 × with 0.2 M ethanolamine (pH 8.0, Sigma, E-6133) for 2 h at room temperature to quench residual DMP. Non-crosslinked IgG antibodies were removed by washing with 3 × 1 mL 0.5% v/v acetic acid (Fisher, A38), 150 mM NaCl (Fisher, S271). The beads were then washed 3 × with ice cold PBS prior to use. Nuclear extracts from xenoestrogen exposed cells (0.1–0.2 mg) were added to 25 μL of uncoupled protein A/G resin and incubated for 30 min to “pre-clear” the extracts prior to IP. The precleared extracts were then adjusted to 1.0 mL with nuclear extraction buffer and added to 25 μL of either anti-ESR1- or IgG-coupled resin. The samples were incubated overnight at 4 °C with end-over-end mixing. The resin was then rinsed 3 × with buffer containing 150 mM NaCl, 50 mM Tris (Fisher, BP152), 10 mM EGTA (Sigma, E-4378), and 0.2% NP40 detergent (Sigma, NP40S) and subsequently washed 3 × with 50 mM ammonium bicarbonate (Fisher, BP2413). Finally, immunoprecipitated ESR1 transcriptional complexes were eluted by adding 50 μL of 0.2% Rapigest SF (Waters Corp., 186,001,860) surfactant in 50 mM ammonium bicarbonate to the beads and boiling at 95 °C. The beads were removed by centrifugation and the supernatant was retained for analysis by LC-MS/MS.

### 2.6. LC-MS/MS

Immunoprecipitated ESR1 complexes (and IgG non-specific binding controls) were digested using Trypsin prior to MS analysis. Supernatants from IP experiments were reduced with 10 mM DTT and alkylated with 200 mM iodoacetamide at room temperature in the dark for 30 min. Sequencing grade trypsin was added to the samples at a loading of ~ 1:50 trypsin:protein (based on original nuclear extract concentration) and samples were digested overnight at 37 °C with shaking. Following digestion, samples were centrifuged at 14,000 x g and the supernatant was adjusted to 1.0% trifluoroacetic acid (TFA) and 2% acetonitrile v/v.

Proteomic analysis of the samples was conducted using a gel-free HPLC-MS/MS approach, with a reversed-phase nanocapillary HPLC separation ($C_{18}$) followed by data-independent MS/MS ($MS^E$) analysis with a Synapt G2 (Waters Corp.) High Definition Mass Spectrometer (quadrupole-time-of-flight).

### 2.7. LC-MS/MS analysis

Mascot was set up to search the SwissProt_2013x database (unknown version, 539,829 entries) also assuming trypsin. IdentityE was searched with a fragment ion mass tolerance of 0.025 Da and a parent ion tolerance of 0.0100 Da. Mascot was searched with a fragment ion mass tolerance of 0.040 Da and a parent ion tolerance of 10.0 PPM. Carbamidomethyl of cysteine was specified in IdentityE and Mascot as a fixed modification. Deamidation of asparagine and glutamine, oxidation of methionine and phosphorylation of serine, threonine and tyrosine were specified in IdentityE as variable modifications. Oxidation of methionine was specified in Mascot as a variable modification. Scaffold (version Scaffold_4.4.3, Proteome Software Inc., Portland, OR) was used to validate MS/MS based peptide and protein identifications. Peptide identifications were accepted if they could be established at greater than 98.0% probability to achieve an FDR less than 1.0%. Peptide Probabilities from IdentityE and Mascot were assigned by the Peptide Prophet algorithm (Keller et al., 2002) with Scaffold delta-mass correction. Peptide Probabilities from IdentityE were assigned by the Scaffold Local FDR algorithm. Protein identifications were accepted if they could be established at greater than 87.0% probability to achieve an FDR less than 5.0% and contained at least 1 identified peptide. Protein Probabilities were assigned by the Protein Prophet algorithm (Nesvizhskii et al., 2003). Proteins that contained similar peptides and could not be differentiated based on MS/MS analysis alone were grouped to satisfy the principles of parsimony. Proteins sharing significant peptide evidence were grouped into clusters. Protein complex predictions and assemblies were performed using the online Search Tool for the Retrieval of Interacting Genes/Proteins (STRING) 10 resource (http://string-db.org) and Subnetwork Enrichment Analysis was performed using Pathway Studio 9.0 (Elsevier). For the analysis, 2 entities (proteins) had to be present in a subnetwork for inclusion and results were limited to 200 subnetworks with best p-value ($p < 0.05$) for enrichment cut-off.

### 2.8. Cross-species analysis

Gene symbols corresponding to the proteins identified in our analysis were obtained using the retrieve/ID mapping option on the UniProt website (uniprot.org/uploadlists). The gene names were converted to their zebrafish orthologs using The Zebrafish Model Organism Database (ZFIN, zfin.org). The Human Gene Database (GeneCards, genecards.org) was used to convert genes not found in The Zebrafish Model Organism Database. STRING was used to identify known and predicted protein–protein interactions using the zebrafish orthologs and specifying *D. rerio* as the organism.

## 3. Results

### 3.1. Xenoestrogens bind ESR1 with varying affinities

We have examined a suite of putative xenoestrogens to quantitatively assess binding to ESR1 using a fluorescence-based competitive ligand binding assay known as fluorescence polarization (FP). We first performed direct binding studies to assess the interaction of ESR1 and a custom-synthesized, fluorescent-labeled probe compound (Fl-$E_1$ fluorescent probe) that was prepared by coupling of fluorescein-5-thiosemicarbazide to the 17-keto position of estrone (Fig. 1). Saturation binding curves for this labeled compound (data not shown)

indicate a binding affinity of 2.3 nM ($K_d$) for the ESR1–Fl-$E_1$ complex, consistent with previous reports and similar to the affinity of the native ligand E2 (Freyberger et al., 2010).

Following validation of the Fl-$E_1$ probe and FP assay, competitive binding curves for 2 putative xenoestrogens were generated based on their ability to displace the fluorescent probe and bind to purified recombinant ESR1-LBD (ligand binding domain) (Fig. 1). In this study, all compounds exhibited specific binding to the ESR1 as indicated by their $IC_{50}$ values and relative binding affinities (RBAs). The antagonist TAM displayed a stronger affinity for ESR1 with an $IC_{50}$ value of 2.8 nM compared to that of E2 (9.5 nM). All other compounds exhibited weak binding relative to the endogenous hormone, E2, (TAM > E2 ≫ GEN > BPA) (Fig. 1).

### 3.2. Xenoestrogens differentially recruit SRC-1 and SRC-3 peptides to the ER complex

Structurally-diverse xenoestrogens may act *via* divergent mechanisms to stimulate estrogen-signaling, including differential, ligand-dependent recruitment of co-regulatory proteins to human ESR1. Upon optimization of experimental parameters, we screened the afore-mentioned xenoestrogens for recruitment activity by the ESR1 using these select peptides. Estradiol was used as a positive control, since its ability to activate and induce recruitment of co-regulators to ESR1 is known. E2 yielded a maximum TR-FRET signal relative to all other compounds in its ability to induce ESR1-SRC interactions (Fig. 3). However, E2 differentially recruited specific peptides and based on the $EC_{50}$ values (Table 2) show the following interaction; SRC-1(3) > SRC-3(3) > SRC-1(2) > SRC-3(2) > SRC-1(1). Estrogen failed to recruit the C-terminal peptide of SRC-1 and SRC-3(3). As anticipated, the antagonist TAM did not recruit any of the co-regulator peptides which is consistent with the lack of binding affinity of this compound to ESR1 determined by the FP assay. BPA failed to induce interaction of the receptor with SRC-3 peptides, but did induce recruitment of two SRC-1 derived peptides (SRC-1(2) and SRC-1(3)).

Perhaps the most interesting result for the compounds studied was that of GEN, which variably recruited SRC-1 and -3 peptides but generated a maximum TR-FRET signal for SRC-3(1). In fact, all three SRC-3 peptides were recruited to the complex by GEN whereas only SRC-3 (2 and 3) were recruited by E2. BPA failed to recruit any of the SRC-3 peptides. Overall, SRC recruitment profiles were highly ligand specific.

### 3.3. E2 and xenoestrogens differentially recruit co-regulatory proteins to activated ESR1-transcriptional complexes

Proteomic analysis of MCF-7 nuclear complexes immunoprecipitated using anti-ESR1 antibodies after xenoestrogen exposure resulted in a large number of total protein identifications. Across all samples (including nonspecific-binding IgG controls), 913 unique proteins were identified with at least one high-scoring peptide match. Within those data, 657 proteins were found to have been isolated due to non-specific interaction artifacts in the immunoprecipitation procedure. These proteins were identified in at least one of the five immunoprecipitation control preparations in which nuclear extracts were isolated using mouse IgG crosslinked to protein A/G beads and were considered to be non-interactors (or non-specific interactors) with the ESR1. Veracity of the immunoprecipitation procedure and

the sensitivity of the proteomics assay were illustrated by the fact that the human ER (ESR1, the target of the IP antibody) was identified in all samples which were immunoprecipitated with anti-ESR1 coupled protein A/G beads. Of the proteins that were not detected in IgG controls, 152 were identified in at least one replicate of DMSO carrier controls, 135 in at least one replicate of the E2-treated cells, 37 in at least one replicate of BPA-treated cells, and 15 in at least one replicate of the GEN-treated cells. As illustrated in Fig. 4, there was considerable overlap in the identity of ESR1 transcriptional complex members present in xenoestrogen-treated MCF-7 cells; however a number of treatment-specific proteins were observed for E2, GEN, and BPA. The list of proteins identified from xenoestrogen-treated proteins in this manner is presented in Table 3.

### 3.4. Proteins recruited in response to E2 and xenoestrogen exposure share a number of known and unknown relationships with ESR1

STRING software was used to identify proteins sharing known protein–protein interactions based on the published literature. A number of the identified proteins were determined to share primary relationships with ESR1 (Fig. 5). E2 recruited six proteins sharing known primary interactions with ESR1; Catenin beta-1 (*CTNNB1*), Guanine nucleotide-binding protein G(q) subunit alpha (*GNAQ*), Histone-binding protein *RBBP7* (*RBBP7*), TUBB2A protein (*TUBB2A*), Proteasome activator complex subunit 3 (*PSME3*), and Splicing factor 1 (*SF1*). BPA recruited three proteins with known primary interactions: Connective tissue growth factor (*CTGF*), Nucleoside diphosphate kinase A (*NME1*), Tubulin alpha-8 chain (*TUBA8*). Genistein recruited one protein with known primary interactions, Heat shock protein HSP 90-beta (*HSP90AB1*). The proteins sharing known primary interactions with ESR1 also share relationships with a number of other proteins identified in our analysis as determined by STRING software and may interact with ESR1 *via* tethering mechanisms. Proteins that do not share known relationships with ESR1 based on the published literature represent potential novel interactors and co-regulatory proteins. Interestingly, a larger percentage of the proteins identified in the BPA and genistein exposed groups did not share any relationship with ESR1 either through direct interactions or via secondary interactions (70% and 60%, respectively) compared to E2 (42%).

### 3.5. E2 and BPA recruited proteins involved in similar cellular processes while genistein recruited proteins involved in unique cellular processes

Subnetwork enrichment analysis was performed using Pathway Studio to identify cellular processes that were enriched with proteins identified in each exposure group (Fig. 6). All three treatments caused enrichment of proteins involved in cell growth. A high degree of overlap existed in cell processes enriched after exposure to E2 and BPA and included apoptosis, cell adhesion, cell cycle, cell death, cell differentiation, cell growth, and cell migration. E2 specifically caused enrichment of proteins involved in endocytosis and mitosis while BPA specifically caused enrichment of proteins involved in cell survival, and S phase. Both BPA and genistein caused enrichment of oxidative stress proteins and both E2 and genistein caused enrichment of RNA splicing proteins. Cell processes specifically enriched by genistein included mitochondrial damage, DNA damage checkpoint, fatty acid oxidation, gene silencing, lipid transport, oncogenesis, and response to oxidative stress. The cellular process enriched with the largest percentage of proteins recruited to ESR1 in response to E2

and BPA were apoptosis and cell differentiation whereas genistein most recruited proteins involved in cell growth and RNA splicing.

### 3.6. Fewer protein–protein interactions exist between zebrafish (D. rerio) orthologs of esr1 and other proteins identified in our co-immunoprecipitation analysis

The proteins identified in the E2 exposed group were converted to their zebrafish orthologs and an interaction network was constructed based on known and inferred protein–protein interactions using STRING analysis. In all, 67 of the 76 proteins identified in the E2 group were successfully mapped to zebrafish orthologs using ZFIN and GeneCards. Of the 67 proteins, 64 were mapped in the zebrafish STRING database and used to construct the interaction network (Fig. 7). Results of the *in silico* analysis revealed that ten proteins shared known or inferred relationships with esr1 either directly (primary) or indirectly (secondary). This accounted for 15.6% of mapped proteins while 37 of the 64 proteins successfully mapped to their zebrafish orthologs shared known or inferred relationships with ESR1 in the human STRING database and accounted for 57.8%. These results are detailed in Table 4.

## 4. Discussion

In the classical model of ER action, the endogenous hormone E2 mediates transactivation in the nucleus. A cascade of signaling events occur such that co-regulatory proteins (co-activators or co-repressors) are recruited to a macromolecular transcriptional complex, the composition and stoichiometry of which is dependent on the conformation adopted by the ER when bound to agonist or antagonist ligands (Paige et al., 1999; O'Malley, 2005). While the influence of native estrogens such as E2 on these transactivation events has been well-studied, the role of xenoestrogens on this system is poorly defined in comparison. Since xenoestrogens have the ability to bind to ER and are thought to cause variable conformational changes in the protein, it is possible that differential recruitment of co-regulators may occur. This xenoestrogen-specific recruitment may have consequences on downstream transcription of gene targets by directing the complex to alternate promoter elements.

To begin to tease apart ligand-specific effects on human ESR1, we performed binding assays to measure binding affinities of various ESR1 ligands for the receptor. In lieu of performing radioligand binding studies, we employed a high-throughput fluorescence polarization (FP) assay to screen the select xenoestrogens for their ability to bind human ESR1. Calculated RBAs, compared to E2 set at 100%, indicated weak binding of most ligands tested except TAM. These values correspond to the range of RBAs (or $IC_{50}$ values) that have been previously reported based on radioligand, polarization anisotropy and fluorescence-based assays (Table 1) (Bolger et al., 1998; Kuiper et al., 1998a; Kuiper et al., 1998b; Matthews et al., 2000; Nikov et al., 2000; Parker et al., 2000; Nikov et al., 2001; Kuramitz et al., 2002; Ohno et al., 2002; Ohno et al., 2003; Mueller et al., 2004; Olsen et al., 2005; Matsui, 2007; Freyberger et al., 2010; Kwok and Cheung, 2010; McLachlan et al., 2011). In general, our assay produces slightly increased affinities for tested xenoestrogen ligands compared to radioligand assays, a result that is likely due to the fact that FP is a homogeneous assay. This alleviates concern over kinetically-limited binding and hysteretic conditions that may impact

results from heterogeneous assays such as the radioligand binding assay. This observation is consistent with RBAs gained from contemporary fluorescent-based techniques, where higher values for BPA, NP and GEN have been reported compared to standard radioligand assays (Ohno et al., 2003). Like other FP assays, ours is fast, convenient, and ideal for high-throughput screening but does have the limitation of not utilizing the entire receptor. It has the additional advantage of using a novel fluorescent ligand ($F\text{-}E_1$) that is easily prepared in high-yield by direct reaction of estrone with commercially-available fluorescein thiosemicarbazide and subsequent purification by reversed-phase HPLC. Overall, our results illustrate the utility of this method for high-fidelity screening of molecular binding to protein receptor targets.

It is well documented that xenoestrogens generally have low affinity for ERs relative to native and therapeutic ligands; however, transcriptional activation at various response elements does not necessarily correlate with the strength of ER binding (Kuiper et al., 1998a). In addition, RBAs do not differentiate between agonist and antagonist abilities, most clearly demonstrated by TAM and other SERM compounds. This is also the case ligandssuch as GEN, which has a greater RBA to human estrogen receptor β (ESR2) (~87%) but activation potential can be greater for ESR1 in transactivation assays (Kuiper et al., 1998a). That same study showed that despite a greater RBA of certain OH-PCBs for the ERs compared to other xenoestrogens, similar activation of the receptors was not refiected in transactivation assays.

A number of studies have addressed the potential role of differential recruitment of co-regulatory proteins to explain ligand and cell type-specific effects of E2 by focusing on the p160 family of coactivators, specifically SRCs (SRC-1,-2,-3) (Chang et al., 1999a; Mc Ilroy et al., 2006; Suzuki et al., 2007). Fewer studies have focused on the role of these coactivators in ligand-specific transcriptional activation by ESR1, particularly with respect to differential cellular responses to xenoestrogens. As such, using TR-FRET, we demonstrate ligand-specific recruitment profiles of SRC-1 and SRC-3 peptides by E2, TAM, GEN and BPA. TAM did not induce recruitment of any of the tested SRC peptides to the ESR1 complex, indicating it may antagonize receptor activity by inducing a conformational change not suitable for binding of co-activator proteins. These compounds may in fact act as allosteric antagonists by recruiting co-repressor proteins rather than co-activators as would be expected with TAM in certain tissues. None of the ligands tested recruited all peptides nor were the profiles identical to E2. For example, all centrally located SRC-1 peptides were recruited by E2 while GEN and BPA were unable to induce recruitment of all three distinct LXXLL motif-containing peptides. Conversely, GEN weakly induced SRC-1(4) interaction with the ER, but this relation was not induced by E2. These results are not in complete agreement with a previous report where the complete RID of SRC-1 was recruited to ESR1 by GEN and BPA with $K_d$ values of 21 nM and 104 nM, respectively (Suzuki et al., 2007).Perhaps differential sensitivity between the assays may account for this discrepancy. The moderate binding of SRC-1(2) to the ESR1 induced by GEN and BPA suggest that this region of the co-regulator may be positioned for maximal interaction as a result of ligand directed conformational change of the receptor.

Recently there has been increased interest in shifting from a targeted analysis of co-regulatory protein recruitment to a global analysis of the ER transcriptional complex and protein–protein interactions therein. One method requires isolating overexpressed ER transcriptional complexes using an immobilized estrogen response element on a sepharose column (Nalvarte et al., 2010). Another method relies on immunoprecipitation of bait protein and subsequent release of complex members in lysis buffer and identification by mass spectrometry (Ewing et al., 2007). Both methods require the use of recombinant bait proteins which is problematic as the overexpression of bait protein can lead to biases in the results by increasing the identification of false positives (Malovannaya et al., 2010). As such, we developed a functional proteomic method to isolate intact co-regulatory proteins bound to endogenous human ESR1 by co-immunoprecipitation using an anti-ESR1 IgG in MCF-7 cells. We used our method to identify proteins recruited to ESR1 after exposure to E2, GEN, and BPA. The analysis was sensitive enough to identify the ESR1 in each replicate from every treatment showing that it is possible to isolate transcriptional complexes from human cell culture without overexpressing the target protein. This allowed us to circumvent problems associated with abnormally high levels of bait protein (Malovannaya et al., 2010). E2 recruited the greatest number of proteins to ESR1 followed by BPA and then genistein. These results are in contrast to the SRC-1/3 peptide recruitment experiments which indicated that genistein recruited more SRC-1/3 peptides than BPA (Table 2) and highlight ligand specific responses. In support of this notion, little overlap in recruited proteins among the treatment groups occurred (Fig. 4) suggesting that each ligand induces a unique conformational change that favors the recruitment of different co-regulatory proteins.

Interestingly, SRC-3 was not among the identified proteins recruited after 3.5 h of ligand induction even though SRC-3 peptides were shown to be recruited by E2 and GEN in the TR-FRET experiments. This result was surprising as other groups have reported high concentrations of SRC-3 in MCF-7 cells (Thenot et al., 1999) and have successfully co-immunoprecipitated SRC-3 with ESR1 antibodies after 3.5 h of E2 induction (Tikkanen et al., 2000a). The discrepancy could be a result of variable stringencies in co-immunoprecipitation methods or the transient and labile nature of co-regulator interaction. Further, we potentially identified some nonspecific interactors in our analysis that could have been eliminated by adding an ultracentrifugation step after primary antibody incubation (Malovannaya et al., 2010). Nonetheless, the identification of a suite of known and previously unknown co-regulatory proteins in our analysis confirms the robustness of our mass spectrometric identification method.

Next, we sought to identify relationships between proteins recruited to human ESR1 in response to each ligand using STRING 10. This analysis revealed that a number of the identified proteins share known relationships with ESR1 through direct interactions while others share secondary relationships via interactions through other proteins (Fig. 5). For example, we identified Catenin beta-1 (CTNNB1), a protein sharing known primary relationships with ESR1, in E2 exposed cells. CTNNB1 is the downstream regulator of the Wnt pathway and an indiscriminate nuclear receptor coactivator that binds LXXLL motifs and is especially important in androgen receptor activity and cellular proliferation (Mulholland et al., 2005). It has been found to form a complex with ESR1 and facilitate transcription in the brain (Varea et al., 2009). Splicing factor 1 (SF1), also identified in the

E2 exposed group, shares a direct relationship with ESR1 and affects gene transactivation and pre-mRNA splicing activities of CTNNB1 complex in colorectal cancer (Shitashige et al., 2007). The identification of CTNNB1 and SF1 in the E2 group suggests that E2 may modulate components of the Wnt signaling pathway through recruitment of Wnt-related co-regulatory proteins to ESR1 in MCF-7 cells.

We also identified potential novel ESR1 co-regulatory proteins such as Filamin-C (FLNC), an actin binding protein that is suggested to function as an androgen receptor coactivator mediating the growth and differentiation of muscle cells (Ting and Chang, 2008). While no evidence for a direct interaction between ESR1 and FLNC was found in the STRING analysis, the identification of FLNC in the E2 exposed group suggests that it might function as a previously unknown estrogen receptor co-regulatory protein and interact with ESR1 through direct or tethering mechanisms thereby coordinating regulation of the cytoskeleton. Identification of the structural protein Vimentin in the E2 group further suggests a role for ESR1 in regulating cytoskeletal architecture (Fig. 5).

STRING analysis also resulted in a number of interesting observations in the xenoestrogen exposed groups. Both E2 and BPA (but not genistein) recruited Cadherin-1 (CDH1), which exhibited a primary relationship with ESR1 and is involved in maintaining the epithelial phenotype of cells and its expression is regulated by ligand-independent actions of ESR1 (Cardamone et al., 2009). The identification of CDH1 suggests that E2 and BPA may influence cellular phenotype via inducing an interaction between ESR1 and this protein. CDH1 was also identified in the DMSO group in our analysis; however, this is not surprising as previous studies have indicated a ligand-independent role for ESR1 in maintaining the epithelial phenotype through modulation of CDH1 expression that is repressed upon ligand-binding thereby promoting an exchange of coactivators for corepressors (Cardamone et al., 2009).

Of note is the BPA-specific recruitment of connective tissue growth factor (CTGF), a matricellular protein involved in numerous biological processes include wound healing, proliferation, and cell–cell adhesion and migration (Hall-Glenn and Lyons, 2011). Previous studies have indicated that BPA is capable of increasing cell proliferation through up-regulation of CTGF expression via G protein-coupled estrogen receptor (GPER) in breast cancer fibroblasts (Pupo et al., 2012). Our results suggest another possible mechanism of BPA-induced regulation of CTGF activity through interactions with ESR1. Interestingly, E2, BPA, and genistein but not vehicle control induced an interaction between ESR1 and transmembrane protein 205 which has been implicated in resistance to the chemotherapeutic cisplatin *in vitro* (Shen et al., 2010). Future studies should investigate a role for ESR1 in modulating cisplatin resistance.

Through a subnetwork enrichment analysis of proteins identified in each treatment group we identified severl functional relationships. Not surprisingly, a number of the proteins recruited to ESR1 in response to E2 and xenoestrogen binding were involved in apoptosis, cell growth, and cell cycle (Fig. 6). ESR1 is known to influence these processes in MCF-7 cells (Brünner et al., 1989; Wang and Phang, 1995; Mawson et al., 2005) and may be influenced by contaminant exposure (Hsieh et al., 1998; Diel et al., 2002). E2 has also been shown to

influence the differentiation of other cell types such as endothelial progenitor cells (Imanishi et al., 2005) and osteoblasts (Qu et al., 1998). While it is not surprising that these processes were found to be enriched with proteins identified in our analysis, our assay was not quantitative thus we cannot determine whether these processes were up or down-regulated.

We also identified a number of xenoestrogen exposure-specific effects. For example, BPA and genistein but not E2 recruited a large percentage of proteins involved in oxidative stress which represents a possible target of xenoestrogen action caused by differential co-regulatory protein recruitment. This is in accordance with previous studies indicating an association between BPA exposure and oxidative stress in postmenopausal women (Yang et al., 2009), and that GEN up-regulated the expression of genes involved in oxidative stress in MCF-7 cells (Borrás et al., 2006). Another striking observation of the subnetwork enrichment analysis was the highly discrepant enrichment of cellular processes by genistein compared to E2 and BPA. Genistein specifically induced recruitment of proteins involved in mitochondrial damage, fatty acid oxidation, lipid transport, and DNA damage checkpoint (Fig. 6).

We expect our co-immunoprecipitation method to be useful in investigating the recruitment of co-regulatory proteins to ligand-activated ESR1 in other species. Because ER signaling is fairly conserved across species (Lam et al., 2011), a comparative approach would increase our understanding of the complex mechanisms of action of endocrine disrupting contaminants in both human and aquatic targets. The observation that BPA and genistein are able to bind to ERs, albeit with lower affinity than E2, and influence reproductive endpoints in fish species (Scholz and Mayer, 2008) further highlights the importance of studying their interactions with the ERs. In fact, it has been found that various fish species respond differently to exposure to environmental estrogens (Miyagawa et al., 2014) which suggests that variable expression of co-regulatory proteins may play a role in such responses in addition to amino acid substitutions in ER sequences across species. Most studies to date have focused on a small suite of co-regulatory proteins such as TIF2 (Tan et al., 2005) and COUP-TFI and COUP-TFII (Métivier et al., 2000), but no reports have utilized a global approach to examine the influence of differential co-regulatory protein recruitment on molecular responses in fish exposed to xenoestrogens.

As a first-pass screen of the translatability of our results to an aquatic species, we performed an *in silico* analysis of interactions between putative co-regulatory proteins identified in our functional proteomic analysis and zebrafish esr1. We converted the 76 proteins in our analysis that were recruited to ESR1 in response to E2 binding to their zebrafish orthologs using ZFIN and constructed plausible interaction networks using STRING 10 (Fig. 7). In total, 64 homologous zebrafish proteins were successfully identified and 15.6% exhibited known or inferred interaction with zebrafish esr1 while 57.8% of human orthologs shared an interaction (Table 4). These results are not surprising due to the lack of data regarding co-regulatory protein recruitment of fish ERs, differences in experimental methods, and variable ligand affinity and co-regulatory protein expression across species. It is well accepted that the ligand affinities of various xenoestrogens for ESR1 differ among species such as medaka (*Oryzias latipes*), stickleback, bluegill (*Lepomis macrochirus*), and guppy (*Poecilia reticulata*), and one group showed that constructing esr1 chimeras in which the AF-

containing domains were swapped between the fish species changed the ligand binding affinities and responsiveness of that species to the xenoestrogens (Miyagawa et al., 2014). These data suggest that the structure of the AF-domain can alter ligand binding which has implications for the recruitment and interaction of co-regulatory proteins with the ERs and downstream signaling responses. To be sure, other factors may also contribute to differential ER signaling responses not limited to species-specific amino acid sequences and the presence of multiple ER isoforms. Our co-immunoprecipitation method would be perfectly suited to study differences in recruitment of co-regulatory proteins to esr1 between fish species thereby increasing our basic understanding of ER signaling in fish.

Overall, development of relevant high-throughput screening assays affords us the ability to test and generate ER-interacting ligand and protein profiles that may be predictive of their activity in cell and tissue environments in humans and fish. As transcriptional complexes require intricate protein–protein and protein–DNA interactions, the need for identifying these complexes in a more comprehensive manner and assessing alternate promoter sites is increasingly acute in understanding ER signaling. Herein we have shown that various ESR1 agonists and antagonists exhibit variable binding affinities and that these binding affinities do not necessarily correlate with co-regulatory protein recruitment profiles, an observation that has puzzled investigators and highlights the complexity of hormonal signaling (Kuiper et al., 1998a; Chang et al., 1999b; O'Malley, 2005). Data presented here offer possible mechanisms in support of this observation as it relates to both known (SRC-3) and unknown ER co-regulatory proteins and xenoestrogens. These data also suggest that investigating recruitment of select peptides derived from known co-regulatory proteins is not an accurate predictor of the recruitment of intact, endogenous proteins to ESR1 by xenoestrogens as genistein exhibited the greatest recruitment of SRC-3 peptides, excluding E2, but recruited the fewest intact, endogenous proteins to ESR1. Further, the select suite of intact, endogenous proteins recruited to ESR1 in response to each ligand increases our understanding of the cellular consequences of xenoestrogen exposure that may have relevance for both mammalian and fish species.

## Acknowledgments

This work was supported by NIH grant number 1R21ES16617.

## References

Adamczyk M, Reddy RE, Yu Z. Synthesis of a novel fluorescent probe for estrogen receptor. Bioorg. Med. Chem. Lett. 2002; 12:1283–1285. [PubMed: 11965371]

Bergman Å, Heindel J, Jobling S, Kidd K, Zoeller RT. State-of-the-science of endocrine disrupting chemicals, 2012. Toxicol. Lett. 2012; 211:S3.

Bolger R, Wiese TE, Ervin K, Nestich S, Checovich W. Rapid screening of environmental chemicals for estrogen receptor binding capacity. Environ. Health Perspect. 1998; 106:551–557. [PubMed: 9721254]

Borrás C, Gambini J, Gómez-Cabrera MC, Sastre J, Pallardó FV, Mann GE, Viña J. Genistein, a soy isoflavone, up-regulates expression of antioxidant genes: involvement of estrogen receptors, ERK1/2, and NFκB. FASEB J. 2006; 20:2136–2138. [PubMed: 16966488]

Brünner N, Bronzert D, Vindeløv LL, Rygaard K, Spang-Thomsen M, Lippman ME. Effect on growth and cell cycle kinetics of estradiol and tamoxifen on MCF-7 human breast cancer cells grown in vitro and in nude mice. Cancer Res. 1989; 49:1515–1520. [PubMed: 2924304]

Cardamone MD, Bardella C, Gutierrez A, Di Croce L, Rosenfeld MG, Di Renzo MF, De Bortoli M. ERα as ligand-independent activator of CDH-1 regulates determination and maintenance of epithelial morphology in breast cancer cells. Proc. Natl. Acad. Sci. 2009; 106:7420–7425. [PubMed: 19383788]

Chang, C.-y.; Norris, JD.; Grøn, H.; Paige, LA.; Hamilton, PT.; Kenan, DJ.; Fowlkes, D.; McDonnell, DP. Dissection of the LXXLL nuclear receptor–coactivator interaction motif using combinatorial peptide libraries: discovery of peptide antagonists of estrogen receptors α and β. Mol. Cell. Biol. 1999a; 19:8226–8239. [PubMed: 10567548]

Chang C, Norris JD, Gron H, Paige LA, Hamilton PT, Kenan DJ, Fowlkes D, McDonnell DP. Dissection of the LXXLL nuclear receptor–coactivator interaction motif using combinatorial peptide libraries: discovery of peptide antagonists of estrogen receptors alpha and beta. Mol. Cell. Biol. 1999b; 19:8226–8239. [PubMed: 10567548]

Dahlman-Wright K, Cavailles V, Fuqua SA, Jordan VC, Katzenellenbogen JA, Korach KS, Maggi A, Muramatsu M, Parker MG, Gustafsson J-Å. International union of pharmacology. LXIV. Estrogen receptors. Pharmacol. Rev. 2006; 58:773–781. [PubMed: 17132854]

Diel P, Olff S, Schmidt S, Michna H. Effects of the environmental estrogens bisphenol A, o, p′-DDT, p-tert-octylphenol and coumestrol on apoptosis induction, cell proliferation and the expression of estrogen sensitive molecular parameters in the human breast cancer cell line MCF-7. J. Steroid Biochem. Mol. Biol. 2002; 80:61–70. [PubMed: 11867264]

Edwards DP. The role of coactivators and corepressors in the biology and mechanism of action of steroid hormone receptors. J. Mammary Gland Biol. Neoplasia. 2000; 5:307–324. [PubMed: 14973393]

Ewing RM, Chu P, Elisma F, Li H, Taylor P, Climie S, McBroom-Cerajewski L, Robinson MD, O'Connor L, Li M. Large-scale mapping of human protein–protein interactions by mass spectrometry. Mol. Syst. Biol. 2007; 3

Freyberger A, Wilson V, Weimer M, Tan S, Tran HS, Ahr HJ. Assessment of a robust model protocol with accelerated throughput for a human recombinant full length estrogen receptor-alpha binding assay: protocol optimization and intralaboratory assay performance as initial steps towards validation. Reprod. Toxicol. 2010; 30:50–59. [PubMed: 20074635]

González-Arenas A, Hansberg-Pastor V, Hernández-Hernández OT, González-García TK, Henderson-Villalpando J, Lemus-Hernández D, Cruz-Barrios A, Rivas-Suárez M, Camacho-Arroyo I. Estradiol increases cell growth in human astrocytoma cell lines through ERα activation and its interaction with SRC-1 and SRC-3 coactivators. Biochim. Biophys. Acta. 2012; 1823:379–386. [PubMed: 22142990]

Gruber CJ, Tschugguel W, Schneeberger C, Huber JC. Production and actions of estrogens. N. Engl. J. Med. 2002; 346:340–352. [PubMed: 11821512]

Hall JM, Korach KS. Analysis of the molecular mechanisms of human estrogen receptors alpha and beta reveals differential specificity in target promoter regulation by xenoestrogens. J. Biol. Chem. 2002; 277:44455–44461. [PubMed: 12200415]

Hall-Glenn F, Lyons KM. Roles for CCN2 in normal physiological processes. Cell. Mol. Life Sci. 2011; 68:3209–3217. [PubMed: 21858450]

Hsieh CY, Santell RC, Haslam SZ, Helferich WG. Estrogenic effects of genistein on the growth of estrogen receptor-positive human breast cancer (MCF-7) cells in vitro and in vivo. Cancer Res. 1998; 58:3833–3838. [PubMed: 9731492]

Imanishi T, Kobayashi K, Hano T, Nishio I. Effect of estrogen on differentiation and senescence in endothelial progenitor cells derived from bone marrow in spontaneously hypertensive rats. Hypertens. Res. 2005; 28:763–772. [PubMed: 16419650]

Karmakar S, Foster EA, Smith CL. Unique roles of p160 coactivators for regulation of breast cancer cell proliferation and estrogen receptor-alpha transcriptional activity. Endocrinology. 2009; 150:1588–1596. [PubMed: 19095746]

Keller A, Nesvizhskii A, Kolker E, Aebersold R. An explanation of the Peptide Prophet algorithm developed. Anal. Chem. 2002; 74:5383–5392. [PubMed: 12403597]

Kraichely DM, Sun J, Katzenellenbogen JA, Katzenellenbogen BS. Conformational changes and coactivator recruitment by novel ligands for estrogen receptor-alpha and estrogen receptor-beta: correlations with biological character and distinct differences among SRC coactivator family members. Endocrinology. 2000; 141:3534–3545. [PubMed: 11014206]

Kuiper GG, Lemmen JG, Carlsson B, Corton JC, Safe SH, van der Saag PT, van der Burg B, Gustafsson JA. Interaction of estrogenic chemicals and phytoestrogens with estrogen receptor beta. Endocrinology. 1998a; 139:4252–4263. [PubMed: 9751507]

Kuiper GG, Shughrue PJ, Merchenthaler I, Gustafsson JA. The estrogen receptor beta subtype: a novel mediator of estrogen action in neuroendocrine systems. Front. Neuroendocrinol. 1998b; 19:253–286. [PubMed: 9799586]

Kuramitz H, Natsui J, Sugawara K, Itoh S, Tanaka S. Electrochemical evaluation of the interaction between endocrine disrupter chemicals and estrogen receptor using 17,beta-estradiol labeled with daunomycin. Anal. Chem. 2002; 74:533–538. [PubMed: 11838671]

Kwok KC, Cheung NH. Measuring binding kinetics of ligands with tethered receptors by fluorescence polarization and total internal refiection fluorescence. Anal. Chem. 2010; 82:3819–3825. [PubMed: 20387803]

Labhart P, Karmakar S, Salicru EM, Egan BS, Alexiadis V, O'Malley BW, Smith CL. Identification of target genes in breast cancer cells directly regulated by the SRC-3/AIB1 coactivator. Proc. Natl. Acad. Sci. U. S. A. 2005; 102:1339–1344. [PubMed: 15677324]

Lam SH, Lee SG, Lin CY, Thomsen JS, Fu PY, Murthy KR, Li H, Govindarajan KR, Nick LC, Bourque G. Molecular conservation of estrogen-response associated with cell cycle regulation, hormonal carcinogenesis and cancer in zebrafish and human cancer cell lines. BMC Med. Genet. 2011; 4:41.

Lauritsen KJ, List HJ, Reiter R, Wellstein A, Riegel AT. A role for TGF-beta in estrogen and retinoid mediated regulation of the nuclear receptor coactivator AIB1 in MCF-7 breast cancer cells. Oncogene. 2002; 21:7147–7155. [PubMed: 12370804]

Lee HS, Miyauchi K, Nagata Y, Fukuda R, Sasagawa S, Endoh H, Kato S, Horiuchi H, Takagi M, Ohta A. Employment of the human estrogen receptor beta ligand-binding domain and co-activator SRC1 nuclear receptor-binding domain for the construction of a yeast two-hybrid detection system for endocrine disrupters. J. Biochem. 2002; 131:399–405. [PubMed: 11872169]

Malovannaya A, Li Y, Bulynko Y, Jung SY, Wang Y, Lanz RB, O'Malley BW, Qin J. Streamlined analysis schema for high-throughput identification of endogenous protein complexes. Proc. Natl. Acad. Sci. 2010; 107:2431–2436. [PubMed: 20133760]

Matsui K. Combination of receptor-binding assays and designed mutant receptors for discerning agonists and antagonists. J. Pharm. Biomed. Anal. 2007; 43:822–828. [PubMed: 17141447]

Matthews J, Celius T, Halgren R, Zacharewski T. Differential estrogen receptor binding of estrogenic substances: a species comparison. J. Steroid Biochem. Mol. Biol. 2000; 74:223–234. [PubMed: 11162928]

Mawson A, Lai A, Carroll JS, Sergio CM, Mitchell CJ, Sarcevic B. Estrogen and insulin/IGF-1 cooperatively stimulate cell cycle progression in MCF-7 breast cancer cells through differential regulation of c-Myc and cyclin D1. Mol. Cell. Endocrinol. 2005; 229:161–173. [PubMed: 15607540]

Mc Ilroy M, Fleming FJ, Buggy Y, Hill AD, Young LS. Tamoxifen-induced ER-α–SRC-3 interaction in HER2 positive human breast cancer; a possible mechanism for ER isoform specific recurrence. Endocr. Relat. Cancer. 2006; 13:1135–1145. [PubMed: 17158759]

McBryan J, Theissen SM, Byrne C, Hughes E, Cocchiglia S, Sande S, O'Hara J, Tibbitts P, Hill AD, Young LS. Metastatic progression with resistance to aromatase inhibitors is driven by the steroid receptor coactivator SRC-1. Cancer Res. 2012; 72:548–559. [PubMed: 22108824]

McDonnell DP. The molecular pharmacology of estrogen receptor modulators: implications for the treatment of breast cancer. Clin. Cancer Res. 2005; 11:871 s–877 s.

McDonnell DP, Wijayaratne A, Chang CY, Norris JD. Elucidation of the molecular mechanism of action of selective estrogen receptor modulators. Am. J. Cardiol. 2002; 90:35F–43F. [PubMed: 12088776]

McLachlan MJ, Katzenellenbogen JA, Zhao H. A new fluorescence complementation biosensor for detection of estrogenic compounds. Biotechnol. Bioeng. 2011; 108:2794–2803. [PubMed: 21732327]

Métivier R, Le Dréan Y, Salbert G, Pakdel F. Interplay between liganded and orphan nuclear receptors controls reproductive pathways. Biochem. Cell Biol. 2000; 78:345–358. [PubMed: 10949085]

Miyagawa S, Lange A, Hirakawa I, Tohyama S, Ogino Y, Mizutani T, Kagami Y, Kusano T, Ihara M, Tanaka H. Differing species responsiveness of estrogenic contaminants in fish is conferred by the ligand binding domain of the estrogen receptor. Environ. Sci. Technol. 2014; 48:5254–5263. [PubMed: 24689804]

Mueller SO, Simon S, Chae K, Metzler M, Korach KS. Phytoestrogens and their human metabolites show distinct agonistic and antagonistic properties on estrogen receptor alpha (ERalpha) and ERbeta in human cells. Toxicol. Sci. 2004; 80:14–25. [PubMed: 15084758]

Mulholland DJ, Dedhar S, Coetzee GA, Nelson CC. Interaction of nuclear receptors with the Wnt/β-catenin/Tcf signaling axis: Wnt you like to know? Endocr. Rev. 2005; 26:898–915.

Nalvarte I, Schwend T, Gustafsson J-Å. Proteomics analysis of the estrogen receptor α receptosome. Mol. Cell. Proteomics. 2010; 9:1411–1422. [PubMed: 20348541]

Nesvizhskii AI, Keller A, Kolker E, Aebersold R. A statistical model for identifying proteins by tandem mass spectrometry. Anal. Chem. 2003; 75:4646–4658. [PubMed: 14632076]

Nikov GN, Hopkins NE, Boue S, Alworth WL. Interactions of dietary estrogens with human estrogen receptors and the effect on estrogen receptor-estrogen response element complex formation. Environ. Health Perspect. 2000; 108:867–872. [PubMed: 11017892]

Nikov GN, Eshete M, Rajnarayanan RV, Alworth WL. Interactions of synthetic estrogens with human estrogen receptors. J. Endocrinol. 2001; 170:137–145. [PubMed: 11431146]

Nishikawa J, Saito K, Goto J, Dakeyama F, Matsuo M, Nishihara T. New screening methods for chemicals with hormonal activities using interaction of nuclear hormone receptor with coactivator. Toxicol. Appl. Pharmacol. 1999; 154:76–83. [PubMed: 9882594]

Ohno K, Fukushima T, Santa T, Waizumi N, Tokuyama H, Maeda M, Imai K. Estrogen receptor binding assay method for endocrine disruptors using fluorescence polarization. Anal. Chem. 2002; 74:4391–4396. [PubMed: 12236347]

Ohno K, Suzuki S, Fukushima T, Maeda M, Santa T, Imai K. Study on interactions of endocrine disruptors with estrogen receptor using fluorescence polarization. Analyst. 2003; 128:1091–1096. [PubMed: 12964612]

Okubo T, Yokoyama Y, Kano K, Soya Y, Kano I. Estimation of estrogenic and antiestrogenic activities of selected pesticides by MCF-7 cell proliferation assay. Arch. Environ. Contam. Toxicol. 2004; 46:445–453. [PubMed: 15253041]

Olsen CM, Meussen-Elholm ET, Hongslo JK, Stenersen J, Tollefsen KE. Estrogenic effects of environmental chemicals: an interspecies comparison. Comp. Biochem. Physiol. Toxicol. Pharmacol. 2005; 141:267–274.

O'Malley BW. A life-long search for the molecular pathways of steroid hormone action. Mol. Endocrinol. 2005; 19:1402–1411. [PubMed: 15914709]

Paige LA, Christensen DJ, Gron H, Norris JD, Gottlin EB, Padilla KM, Chang CY, Ballas LM, Hamilton PT, McDonnell DP, Fowlkes DM. Estrogen receptor (ER) modulators each induce distinct conformational changes in ER alpha and ER beta. Proc. Natl. Acad. Sci. U. S. A. 1999; 96:3999–4004. [PubMed: 10097152]

Parker GJ, Law TL, Lenoch FJ, Bolger RE. Development of high throughput screening assays using fluorescence polarization: nuclear receptor-ligand-binding and kinase/phosphatase assays. J. Biomol. Screen. 2000; 5:77–88. [PubMed: 10803607]

Pupo M, Pisano A, Lappano R, Santolla MF, De Francesco EM, Abonante S, Rosano C, Maggiolini M. Bisphenol A induces gene expression changes and proliferative effects through GPER in breast cancer cells and cancer-associated fibroblasts. Environ. Health Perspect. 2012; 120:1177–1182. [PubMed: 22552965]

Qu Q, Perälä-Heape M, Kapanen A, Dahllund J, Salo J, Väänänen H, Härkönen P. Estrogen enhances differentiation of osteoblasts in mouse bone marrow culture. Bone. 1998; 22:201–209. [PubMed: 9514212]

Routledge EJ, White R, Parker MG, Sumpter JP. Differential effects of xenoestrogens on coactivator recruitment by estrogen receptor (ER) alpha and ERbeta. J. Biol. Chem. 2000; 275:35986–35993. [PubMed: 10964929]

Scholz S, Mayer I. Molecular biomarkers of endocrine disruption in small model fish. Mol. Cell. Endocrinol. 2008; 293:57–70. [PubMed: 18619515]

Shang Y, Brown M. Molecular determinants for the tissue specificity of SERMs. Science. 2002; 295:2465–2468. [PubMed: 11923541]

Shanle EK, Xu W. Endocrine disrupting chemicals targeting estrogen receptor signaling: identification and mechanisms of action. Chem. Res. Toxicol. 2010; 24:6–19. [PubMed: 21053929]

Shao W, Keeton EK, McDonnell DP, Brown M. Coactivator AIB1 links estrogen receptor transcriptional activity and stability. Proc. Natl. Acad. Sci. U. S. A. 2004; 101:11599–11604. [PubMed: 15289619]

Shen DW, Ma J, Okabe M, Zhang G, Xia D, Gottesman MM. Elevated expression of TMEM205, a hypothetical membrane protein, is associated with cisplatin resistance. J. Cell. Physiol. 2010; 225:822–828. [PubMed: 20589834]

Shibata H, Spencer TE, Onate SA, Jenster G, Tsai SY, Tsai MJ, O'Malley BW. Role of co-activators and co-repressors in the mechanism of steroid/thyroid receptor action. Recent Prog. Horm. Res. 1997; 52:141–164. (discussion 164-145). [PubMed: 9238851]

Shitashige M, Naishiro Y, Idogawa M, Honda K, Ono M, Hirohashi S, Yamada T. Involvement of splicing factor-1 in β-catenin/T-cell factor-4-mediated gene transactivation and pre-mRNA splicing. Gastroenterology. 2007; 132:1039–1054. [PubMed: 17383426]

Sonnenschein C, Soto AM. An updated review of environmental estrogen and androgen mimics and antagonists. J. Steroid Biochem. Mol. Biol. 1998; 65:143–150. [PubMed: 9699867]

Suzuki S, Nishida S, Ohno K.-i. Santa T. Modulation of coactivator recruitment by cooperative ligand binding to human estrogen receptor α and β. Biol. Pharm. Bull. 2007; 30:1641–1647. [PubMed: 17827713]

Tan J-H, Quek S-I, Chan W-K. Cloning, genomic organization, and expression analysis of zebrafish nuclear receptor coactivator, TIF2. Zebrafish. 2005; 2:33–46. [PubMed: 18248177]

Thenot S, Charpin M, Bonnet S, Cavailles V. Estrogen receptor cofactors expression in breast and endometrial human cancer cells. Mol. Cell. Endocrinol. 1999; 156:85–93. [PubMed: 10612426]

Tikkanen MK, Carter DJ, Harris AM, Le HM, Azorsa DO, Meltzer PS, Murdoch FE. Endogenously expressed estrogen receptor and coactivator AIB1 interact in MCF-7 human breast cancer cells. Proc. Natl. Acad. Sci. 2000a; 97:12536–12540. [PubMed: 11050174]

Tikkanen MK, Carter DJ, Harris AM, Le HM, Azorsa DO, Meltzer PS, Murdoch FE. Endogenously expressed estrogen receptor and coactivator AIB1 interact in MCF-7 human breast cancer cells. Proc. Natl. Acad. Sci. U. S. A. 2000b; 97:12536–12540. [PubMed: 11050174]

Ting H-J, Chang C. Actin associated proteins function as androgen receptor coregulators: an implication of androgen receptor's roles in skeletal muscle. J. Steroid Biochem. Mol. Biol. 2008; 111:157–163. [PubMed: 18590822]

Varea O, Garrido JJ, Dopazo A, Mendez P, Garcia-Segura LM, Wandosell F. Estradiol activates beta-catenin dependent transcription in neurons. PLoS One. 2009; 4:e5153. [PubMed: 19360103]

Wang TT, Phang JM. Effects of estrogen on apoptotic pathways in human breast cancer cell line MCF-7. Cancer Res. 1995; 55:2487–2489. [PubMed: 7780952]

Wong CW, Komm B, Cheskis BJ. Structure–function evaluation of ER alpha and beta interplay with SRC family coactivators. ER selective ligands. Biochemistry. 2001; 40:6756–6765. [PubMed: 11389589]

Xu J, Li Q. Review of the in vivo functions of the p160 steroid receptor coactivator family. Mol. Endocrinol. 2003; 17:1681–1692. [PubMed: 12805412]

Yang YJ, Hong Y-C, Oh S-Y, Park M-S, Kim H, Leem J-H, Ha E-H. Bisphenol A exposure is associated with oxidative stress and inflammation in postmenopausal women. Environ. Res. 2009; 109:797–801. [PubMed: 19464675]

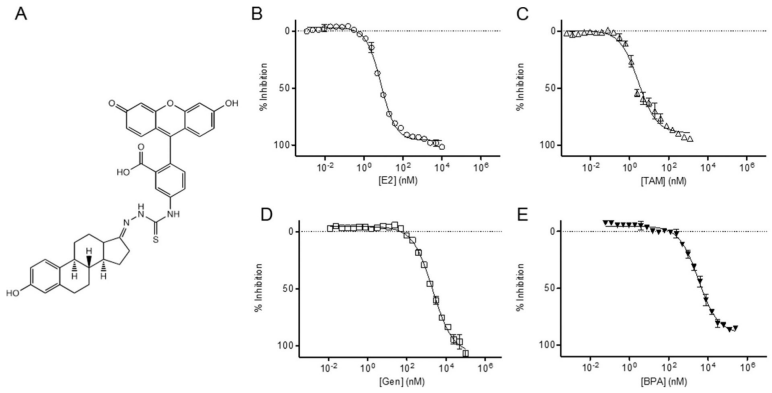


**Fig. 1.**

(A) Chemical structure of the fluorescent estrogen (F-E1) conjugate used in fluorescence polarization competitive ligand binding studies with the human estrogen receptor α. This synthetic probe was prepared by labeling of estrone at the 17-position with fluorescein thiosemicarbazide. (B–E) Binding curves for E2, TAM, BPA, and GEN, respectively, to ESR1 using a fluorescence polarization assay after 1 h incubation in the dark at room temperature. Fluorescence polarization (FP) was measured on a Biotek Synergy H1 spectrophotometer using an excitation wavelength of 485 nm and emission wavelength of 525 nm. FP was converted to percent inhibition ($I_{\%} = (A_0 - A) / (A_0 - A_{100}) * 100$) where A = absorbance and plotted against concentration of ligand using SigmaPlot 11 (Systat Software, Inc., San Jose, CA). Curves were fit by transforming the x-axis to a logarithmic scale. Concentrations (nM) of each ligand are plotted as log concentration compared to % inhibition (n = 3).

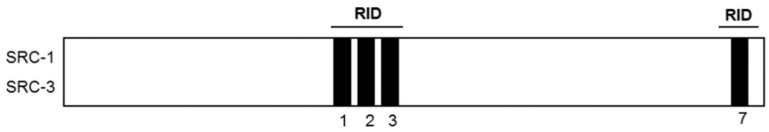


| | Peptide | Sequence | Amino acids | Domain | RID # |
|---|---|---|---|---|---|
| SRC-1 | 1 | KYSQTSHK**LVQLL**TTTAEQL | 625-645 | centrally located RID | 1 |
| | 2 | LTARHKI**LHRLL**QEGSPSD | 683-701 | centrally located RID | 2 |
| | 3 | ESKDHQ L**LRYLL**DKDEKDL | 742-760 | centrally located RID | 3 |
| | 4 | GPQTPQAQQKSL**LQQLL**TE | 1423-1441 | C-terminus RID | 7 |
| SRC-3 | 1 | ESKGHKK**LLQLL**TCSSDDR | 614-632 | centrally located RID | 1 |
| | 2 | LQEKHRI**LHKLL**QNGNSPA | 678-696 | centrally located RID | 2 |
| | 3 | KKENNAL**LRYLL**DRDDPSD | 731-749 | centrally located RID | 3 |

RID = receptor-interacting domain (nuclear receptor box)

**Fig. 2.**

General SRC protein box schematic representing the seven regions containing LXXLL motifs located within the receptor-interacting and activation domains (RID) (adapted from (Edwards, 2000) and SRC peptides screened for recruitment to the ESR1 using TR-FRET with their respective sequences and domain locations.

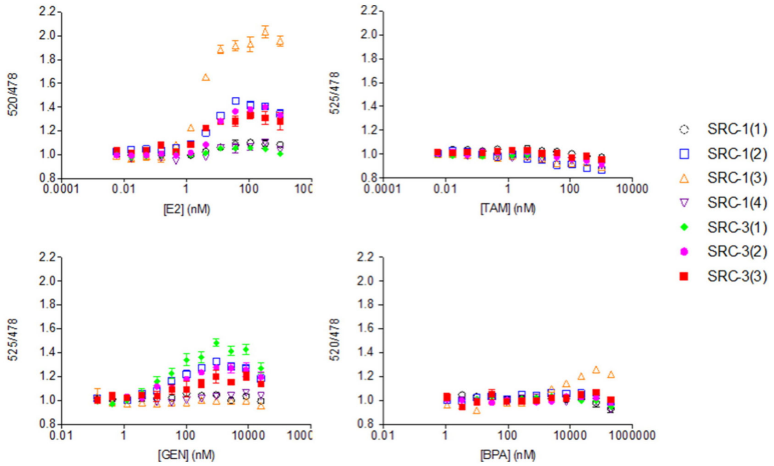


**Fig. 3.**

ESR1 ligands differentially recruit SRC-1 and SRC-3 co-regulatory peptides to the human ESR1. Recruitment was measured using time resolved fluorescent resonance energy transfer after 1 h incubation at room temperature. Recruitment curves are presented as the ratio of fluorescent units (520 nm/478 nm) emitted after excitation at 340 nm versus twelve concentrations (nM) of each ligand. Points indicate average fluorescence ratio of each dose (n = 4). Dose–response curves were generated by plotting emission ratios (y axis) against ligand concentration (x axis) using SigmaPlot 11 (Systat Software, Inc., San Jose, CA). Curves were analyzed by transforming the x-axis to a logarithmic scale and applying a nonlinear regression curve using a sigmoidal-dose response with variable slope using SigmaPlot 11.

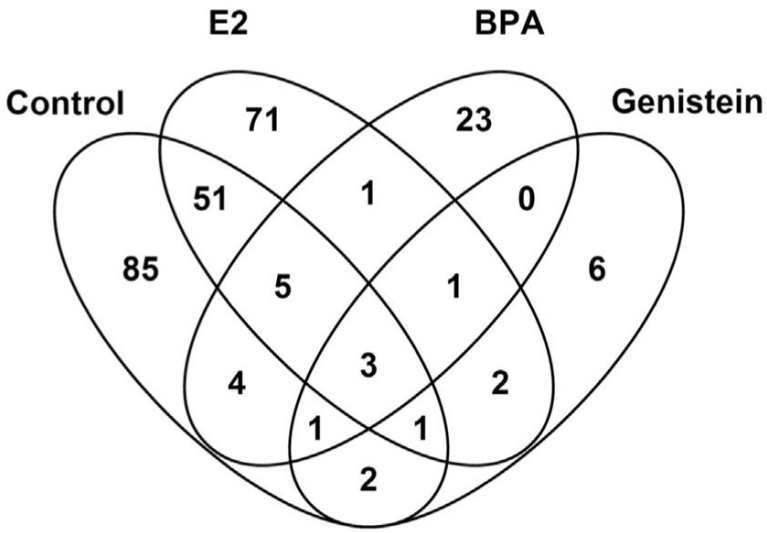


**Fig. 4.**

Estrogen receptor α (ESR1) ligands differentially recruit proteins to ESR1. Venn diagram depicting proteins identified in at least one replicate ESR1 transcriptional complex isolated from MCF-7 nuclear extracts after exposure 10 nM 17β-estradiol (E2), 1 μM bisphenol-A (BPA), 1 μM genistein, or DMSO carrier-control (Control) for a period of 3.5 h ($n \geq 3$). Only proteins that were not observed in IgG nonspecific binding immunoprecipitation controls are represented.

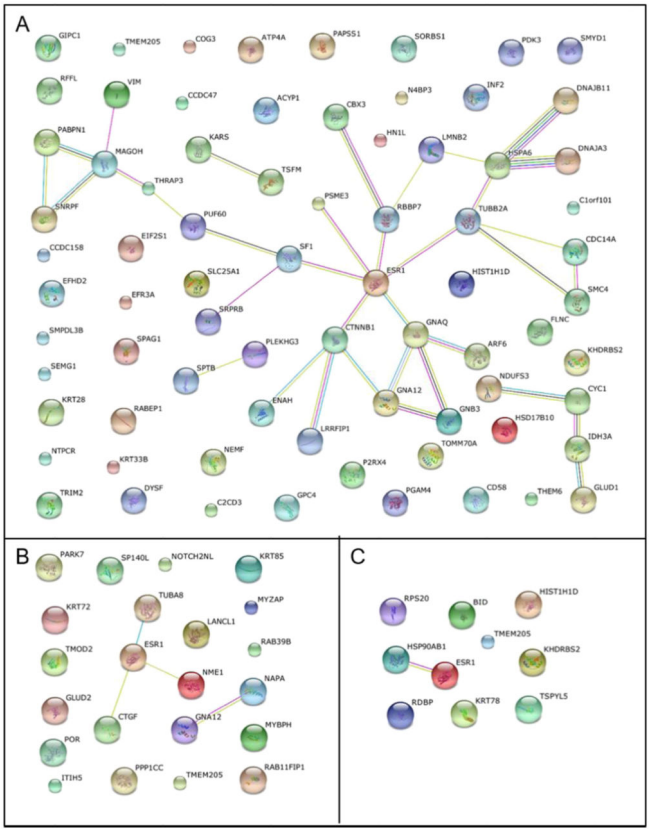


**Fig. 5.**

Proteins recruited to ESR1 in response to ESR1 ligands share both known and unknown interactions. String networks depict interactions among putative ESR1 co-regulatory proteins (shown with gene name) bound to ESR1 after 3.5 h exposure to 10 nM 17β-estradiol (A), 1 μM bisphenol-A (B), or 1 μM genistein (C) in MCF-7 cells based on identification of proteins listed in Table 3. Nodes represent individual proteins, and connecting lines denote known (experimentally-derived or inferred) protein–protein interactions reported in the literature. Figure compiled from http://string-db.org.

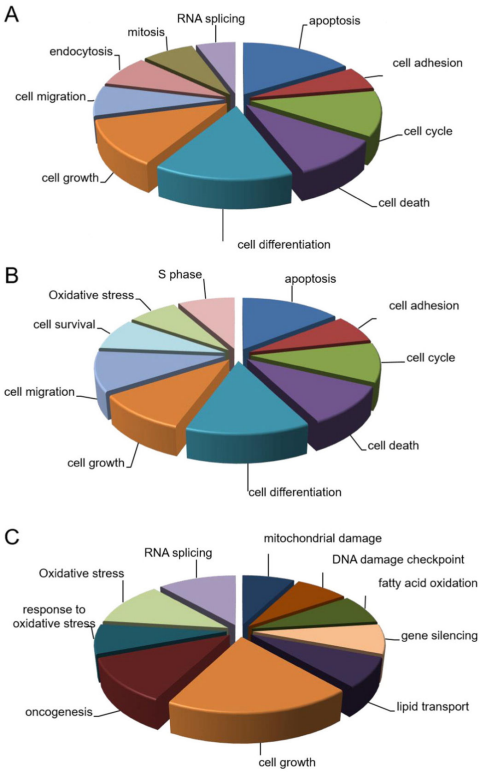


**Fig. 6.**

Pie charts depicting statistically significant ($p < 0.05$) enrichment of cell processes as determined by subnetwork enrichment analysis. Each slice represents the percentage of proteins sorted into each biological process related to the total number of proteins identified in MCF-7 cells exposure to either 10 nM 17β-estradiol (A), 1 μM bisphenol-A (B), or 1 μM genistein (C).

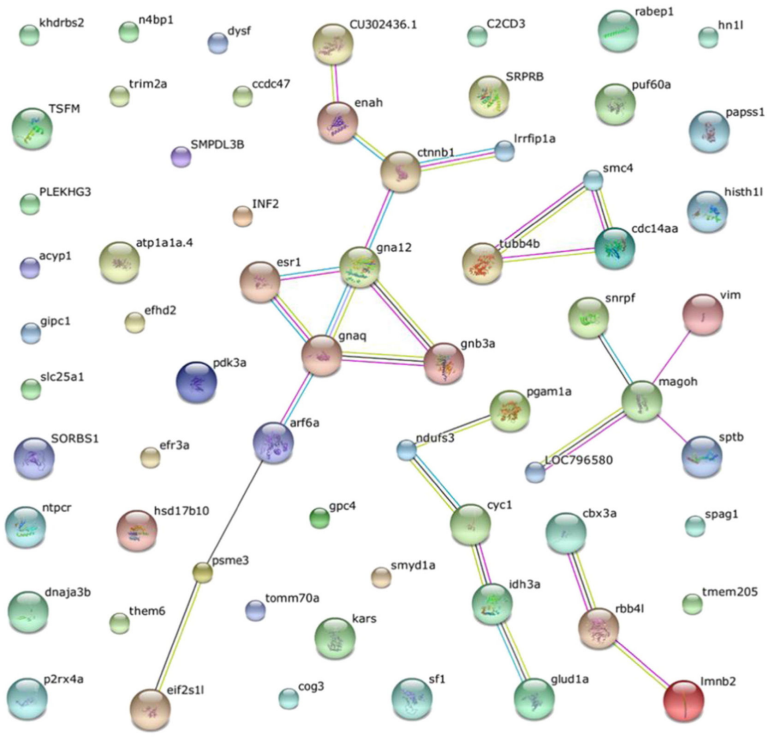


**Fig. 7.**

Summary of interactions among putative zebrafish esr1 co-regulatory proteins (shown with gene name) in the 17β-estradiol (E2) exposed group. Nodes represent individual proteins, and connecting lines denote known (experimentally-derived or inferred) protein–protein interactions reported in the literature. Figure compiled from http://string-db.org.

## Table 1

Relative binding affinities calculated from $IC_{50}$ values of xenoestrogen ligands screened in fluorescence polarization (FP) assay compared to those cited in the literature. Nonlinear regression curves were fit using a sigmoidal-dose response with variable slope to obtain $IC_{50}$ values for the corresponding ligands using SigmaPlot 11.

| Ligand | $IC_{50}$ (nM) | $IC_{50}$ 95% CI (nM) | RBA (%) | Literature RBA (%) |
|---|---|---|---|---|
| 17β-Estradiol | 9.5 | 8.5–10.6 | 100 | – |
| 4-OH-Tamoxifen | 2.8 | 2.0–3.9 | 339 | 4.7–257[a–f] |
| Genistein | 2120 | 1830–2470 | 0.45 | 0.2–16[a,c–f,j,k] |
| Bisphenol-A | 3270 | 2810–3800 | 0.29 | 0.006–0.315[a,d–i] |

[b] Nikov et al. (2001).

[e] Matthews et al. (2000).

[g] Olsen et al. (2005).

[h] Bolger et al. (1998).

[a] Ohno et al. (2003).

[c] Kwok et al. (2010).

[d] Matsui et al. (2006).

[f] Kuiper et al. (1998a, 1998b).

[i] Kuramitz et al. (2002).

[j] Nikov et al. (2000).

[k] Mueller et al. (2004).

## Table 2

Calculated $EC_{50}$ values of each SRC peptide for the ESR1 in response to each ligand in the TR-FRET assays. Dose–response curves were generated by plotting emission ratios (y axis) against ligand concentration (x axis) using SigmaPlot 11 (Systat Software, Inc., San Jose, CA). Curves were analyzed by transforming the x-axis to a logarithmic scale and applying a nonlinear regression curve using a sigmoidal-dose response with variable slope and $EC_{50}$ values calculated using SigmaPlot 11.

| | SRC-1 (nM) | | | | SRC-3 (nM) | | |
|---|---|---|---|---|---|---|---|
| **Ligand** | **(1)** | **(2)** | **(3)** | **(4)** | **(1)** | **(2)** | **(3)** |
| 17β-Estradiol | 8.44 | 5.08 | 2.61 | – | – | 7.19 | 2.74 |
| 4-OH-Tamoxifen | – | – | – | – | – | – | – |
| Genistein | – | 25.0 | – | 511 | 17.0 | 38.8 | 72.4 |
| Bisphenol-A | – | 32.3 | 3230 | – | – | – | – |

## Table 3

Proteins identified from ESR1 transcriptional complexes of MCF-7 cells after exposure to 10 nM 17β-estradiol (E2), 1 μM bisphenol-A (BPA), or 1 μM genistein (GEN) for 3.5 h, excluding proteins identified in control group. Proteins are organized by treatment and number of identifications among triplicate samples within a treatment group (IDs).

| Ligand | UniProt Accession Number | Gene Symbol | Protein Name | Molecular Weight | IDs |
|---|---|---|---|---|---|
| E2 | P03372 | ESR1 | Estrogen receptor | 66 kDa | 3 |
| | Q9UBS4 | DNAJB11 | DnaJ homolog subfamily B member 11[≠] | 41 kDa | 3 |
| | P62330 | ARF6 | ADP-ribosylation factor 6[≠] | 20 kDa | 2 |
| | Q13185 | CBX3 | Chromobox protein homolog 3[≠] | 21 kDa | 2 |
| | P35222 | CTNNB1 | Catenin beta-1[†] | 85 kDa | 2 |
| | P08574 | CYC1 | Cytochrome c1, heme protein, mitochondrial[≠] | 35 kDa | 2 |
| | Q14315 | FLNC | Filamin-C[≠] | 291 kDa | 2 |
| | P50148 | GNAQ | Guanine nucleotide-binding protein G(q) subunit alpha[†] | 42 kDa | 2 |
| | O15049 | N4BP3 | NEDD4-binding protein 3 | 60 kDa | 2 |
| | O75489 | NDUFS3 | NADH dehydrogenase [ubiquinone] iron–sulfur protein 3, mitochondrial[≠] | 30 kDa | 2 |
| | P61289 | PSME3 | Proteasome activator complex subunit 3[†] | 30 kDa | 2 |
| | Q9Y2W1 | THRAP3 | Thyroid hormone receptor-associated protein 3[≠] | 109 kDa | 2 |
| | P07311 | ACYP1 | Acylphosphatase-1 | 11 kDa | 1 |
| | P20648 | ATP4A | Potassium-transporting ATPase alpha chain 1[≠] | 114 kDa | 1 |
| | Q5SY80 | C1orf101 | Uncharacterized protein C1orf101 | 110 kDa | 1 |
| | Q4AC94 | C2CD3 | C2 domain-containing protein 3 | 260 kDa | 1 |
| | Q5M9N0 | CCDC158 | Coiled-coil domain-containing protein 158 | 127 kDa | 1 |
| | Q96A33 | CCDC47 | Coiled-coil domain-containing protein 47 | 56 kDa | 1 |
| | P19256 | CD58 | Lymphocyte function-associated antigen 3 | 28 kDa | 1 |
| | Q9UNH5 | CDC14A | Dual specificity protein phosphatase CDC14A[≠] | 67 kDa | 1 |
| | Q96JB2 | COG3 | Conserved oligomeric Golgi complex subunit 3 | 94 kDa | 1 |
| | Q96EY1 | DNAJA3 | DnaJ homolog subfamily A member 3, mitochondrial[≠] | 52 kDa | 1 |
| | O75923 | DYSF | Dysferlin | 237 kDa | 1 |
| | Q96C19 | EFHD2 | EF-hand domain-containing protein D2 | 27 kDa | 1 |
| | Q14156 | EFR3A | Protein EFR3 homolog A | 93 kDa | 1 |
| | P05198 | EIF2S1 | Eukaryotic translation initiation factor 2 subunit 1[≠] | 36 kDa | 1 |
| | Q8N8S7 | ENAH | Protein enabled homolog[≠] | 67 kDa | 1 |
| | O14908 | GIPC1 | PDZ domain-containing protein GIPC1 | 36 kDa | 1 |
| | P00367 | GLUD1 | Glutamate dehydrogenase 1, mitochondrial[≠] | 61 kDa | 1 |
| | Q03113 | GNA12 | Guanine nucleotide-binding protein subunit alpha-12[≠] | 44 kDa | 1 |

| Ligand | UniProt Accession Number | Gene Symbol | Protein Name | Molecular Weight | IDs |
|---|---|---|---|---|---|
| | P16520 | GNB3 | Guanine nucleotide-binding protein G(I)/G(S)/G(T) subunit beta-3‡ | 37 kDa | 1 |
| | O75487 | GPC4 | Glypican-4‡ | 62 kDa | 1 |
| | P16402 | HIST1H1D | Histone H1.3‡ | 22 kDa | 1 |
| | Q9H910 | HN1L | Hematological and neurological expressed 1-like protein | 20 kDa | 1 |
| | Q99714 | HSD17B10 | 3-hydroxyacyl-CoA dehydrogenase type-2 | 27 kDa | 1 |
| | P48741 | HSPA7 | Putative heat shock 70 kDa protein 7‡ | 40 kDa | 1 |
| | P50213 | IDH3A | Isocitrate dehydrogenase [NAD] subunit alpha, mitochondrial‡ | 40 kDa | 1 |
| | Q27J81 | INF2 | Inverted formin-2 | 136 kDa | 1 |
| | Q15046 | KARS | Lysine–tRNA ligase‡ | 68 kDa | 1 |
| | Q5VWX1 | KHDRBS2 | KH domain-containing, RNA-binding, signal transduction-associated protein 2‡ | 39 kDa | 1 |
| | Q7Z3Y7 | KRT28 | Keratin, type I cytoskeletal 28 | 51 kDa | 1 |
| | Q14525 | KRT33B | Keratin, type I cuticular Ha3-II | 46 kDa | 1 |
| | Q71F78 | LCA10 | Putative lung carcinoma-associated protein 10 | 17 kDa | 1 |
| | Q03252 | LMNB2 | Lamin-B2‡ | 68 kDa | 1 |
| | Q32MZ4 | LRRFIP1 | Leucine-rich repeat flightless-interacting protein 1‡ | 89 kDa | 1 |
| | P61326 | MAGOH | Protein mago nashi homolog‡ | 17 kDa | 1 |
| | O60524 | NEMF | Nuclear export mediator factor NEMF‡ | 123 kDa | 1 |
| | Q9BSD7 | NTPCR | Cancer-related nucleoside-triphosphatase | 21 kDa | 1 |
| | Q99571 | P2RX4 | P2X purinoceptor 4 | 43 kDa | 1 |
| | Q86U42 | PABPN1 | Polyadenylate-binding protein 2‡ | 33 kDa | 1 |
| | O43252 | PAPSS1 | Bifunctional 3′-phosphoadenosine 5′-phosphosulfate synthase 1 | 71 kDa | 1 |
| | Q15120 | PDK3 | [Pyruvate dehydrogenase [lipoamide]] kinase isozyme 3, mitochondrial | 47 kDa | 1 |
| | Q8N0Y7 | PGAM4 | Probable phosphoglycerate mutase 4 | 29 kDa | 1 |
| | A1L390 | PLEKHG3 | Pleckstrin homology domain-containing family G member 3‡ | 134 kDa | 1 |
| | Q9UHX1 | PUF60 | Poly(U)-binding-splicing factor PUF60‡ | 60 kDa | 1 |
| | Q15276 | RABEP1 | Rab GTPase-binding effector protein 1 | 99 kDa | 1 |
| | Q16576 | RBBP7 | Histone-binding protein RBBP7† | 48 kDa | 1 |
| | Q8WZ73 | RFFL | E3 ubiquitin-protein ligase rififylin | 41 kDa | 1 |
| | P04279 | SEMG1 | Semenogelin-1 | 52 kDa | 1 |
| | Q15637 | SF1 | Splicing factor 1† | 68 kDa | 1 |
| | P53007 | SLC25A1 | Tricarboxylate transport protein, mitochondrial | 34 kDa | 1 |
| | Q9NTJ3 | SMC4 | Structural maintenance of chromosomes protein 4‡ | 147 kDa | 1 |
| | Q92485 | SMPDL3B | Acid sphingomyelinase-like phosphodiesterase 3b | 51 kDa | 1 |
| | Q8NB12 | SMYD1 | SET and MYND domain-containing protein 1 | 57 kDa | 1 |
| | P62306 | SNRPF | Small nuclear ribonucleoprotein F‡ | 10 kDa | 1 |

| Ligand | UniProt Accession Number | Gene Symbol | Protein Name | Molecular Weight | IDs |
|---|---|---|---|---|---|
| | Q9BX66 | SORBS1 | Sorbin and SH3 domain-containing protein 1‡ | 143 kDa | 1 |
| | Q07617 | SPAG1 | Sperm-associated antigen 1 | 104 kDa | 1 |
| | P11277 | SPTB | Spectrin beta chain, erythrocytic‡ | 246 kDa | 1 |
| | Q9Y5M8 | SRPRB | Signal recognition particle receptor subunit beta‡ | 30 kDa | 1 |
| | Q8WUY1 | THEM6 | Protein THEM6 | 24 kDa | 1 |
| | Q6UW68 | TMEM205 | Transmembrane protein 205 | 21 kDa | 1 |
| | O94826 | TOMM70A | Mitochondrial import receptor subunit TOM70 | 67 kDa | 1 |
| | Q9C040 | TRIM2 | Tripartite motif-containing protein 2 | 82 kDa | 1 |
| | P43897 | TSFM | Elongation factor Ts, mitochondrial‡ | 35 kDa | 1 |
| | Q13885 | TUBB2A | Tubulin beta-2 A chain† | 50 kDa | 1 |
| | P08670 | VIM | Vimentin‡ | 54 kDa | 1 |
| BPA | P03372 | ESR1 | Estrogen receptor | 66 kDa | 3 |
| | P29279 | CTGF | Connective tissue growth factor† | 38 kDa | 1 |
| | P49448 | GLUD2 | Glutamate dehydrogenase 2, mitochondrial | 61 kDa | 1 |
| | Q03113 | GNA12 | Guanine nucleotide-binding protein subunit alpha-12‡ | 44 kDa | 1 |
| | Q58FG0 | HSP90AA5P | Putative heat shock protein HSP 90-alpha A5 | 39 kDa | 1 |
| | Q86UX2 | ITIH5 | Inter-alpha-trypsin inhibitor heavy chain H5 | 105 kDa | 1 |
| | Q9BW19 | KIFC1 | Kinesin-like protein KIFC1 | 74 kDa | 1 |
| | Q14CN4 | KRT72 | Keratin, type II cytoskeletal 72 | 56 kDa | 1 |
| | P78386 | KRT85 | Keratin, type II cuticular Hb5 | 56 kDa | 1 |
| | O43813 | LANCL1 | LanC-like protein 1 | 45 kDa | 1 |
| | Q13203 | MYBPH | Myosin-binding protein H | 52 kDa | 1 |
| | P0CAP1 | MYZAP | Myocardial zonula adherens protein | 54 kDa | 1 |
| | P54920 | NAPA | Alpha-soluble NSF attachment protein‡ | 33 kDa | 1 |
| | P15531 | NME1 | Nucleoside diphosphate kinase A† | 17 kDa | 1 |
| | Q04721 | NOTCH2 | Neurogenic locus notch homolog protein 2 | 265 kDa | 1 |
| | Q7Z3S9 | NOTCH2NL | Notch homolog 2 N-terminal-like protein | 26 kDa | 1 |
| | Q99497 | PARK7 | Protein DJ-1 | 20 kDa | 1 |
| | P16435 | POR | NADPH–cytochrome P450 reductase | 77 kDa | 1 |
| | P36873 | PPP1CC | Serine/threonine-protein phosphatase PP1-gamma catalytic subunit | 37 kDa | 1 |
| | Q6WKZ4 | RAB11FIP1 | Rab11 family-interacting protein 1 | 137 kDa | 1 |
| | Q96DA2 | RAB39B | Ras-related protein Rab-39B | 25 kDa | 1 |
| | Q9H930 | SP140L | Nuclear body protein SP140-like protein | 67 kDa | 1 |
| | Q6UW68 | TMEM205 | Transmembrane protein 205 | 21 kDa | 1 |
| | Q9NZR1 | TMOD2 | Tropomodulin-2 | 40 kDa | 1 |
| | Q9NY65 | TUBA8 | Tubulin alpha-8 chain† | 50 kDa | 1 |
| GEN | P03372 | ESR1 | Estrogen receptor | 66 kDa | 3 |
| | P55957 | BID | BH3-interacting domain death agonist | 22 kDa | 1 |
| | P16402 | HIST1H1D | Histone H1.3 | 22 kDa | 1 |

| Ligand | UniProt Accession Number | Gene Symbol | Protein Name | Molecular Weight | IDs |
|---|---|---|---|---|---|
| | Q58FF8 | HSP90AB2P | Putative heat shock protein HSP 90-beta 2 † | 44 kDa | 1 |
| | Q5VWX1 | KHDRBS2 | KH domain-containing, RNA-binding, signal transduction-associated protein 2 | 39 kDa | 1 |
| | Q8N1N4 | KRT78 | Keratin, type II cytoskeletal 78 ‡ | 57 kDa | 1 |
| | P18615 | NELFE | Negative elongation factor E | 43 kDa | 1 |
| | P60866 | RPS20 | 40S ribosomal protein S20 | 13 kDa | 1 |
| | Q6UW68 | TMEM205 | Transmembrane protein 205 | 21 kDa | 1 |
| | Q86VY4 | TSPYL5 | Testis-specific Y-encoded-like protein 5 | 45 kDa | 1 |

† after the protein name denotes a primary relationship with ESR1

‡ denotes a secondary relationship as determined by STRING analysis.

**Table 4**

Summary of known and inferred protein-protein interactions between zebrafish esr1 and successfully mapped zebrafish orthologs of putative co-regulatory proteins identified in the 17β-estradiol (E2) exposed group in our study as determined by STRING analysis.

| Human gene symbol | Zebrafish gene symbol | Protein name | Human interaction | Zebrafish interaction |
|---|---|---|---|---|
| ESR1 | esr1 | Estrogen receptor | – | – |
| ACYP1 | acyp1 | Acylphosphatase-1 | | |
| ARF6 | arf6a | ADP-ribosylation factor 6 | ⋕ | ⋕ |
| C2CD3 | c2cd3 | C2 domain-containing protein 3 | | |
| CBX3 | cbx3a | Chromobox protein homolog 3 | | |
| CCDC47 | ccdc47 | Coiled-coil domain-containing protein 47 | | |
| CDC14A | cdc14aa | Dual specificity protein phosphatase CDC14A | | |
| COG3 | cog3 | Conserved oligomeric Golgi complex subunit 3 | | |
| CTNNB1 | ctnnb1 | Catenin beta-1 | † | |
| CYC1 | cyc1 | Cytochrome c1, heme protein, mitochondrial | ⋕ | |
| DNAJA3 | dnaja3b | DnaJ homolog subfamily A member 3, mitochondrial | ⋕ | |
| DYSF | dysf | Dysferlin | | |
| EFHD2 | efhd2 | EF-hand domain-containing protein D2 | | |
| EFR3A | efr3a | Protein EFR3 homolog A | | |
| EIF2S1 | eif2s1a | Eukaryotic translation initiation factor 2 subunit 1 | ⋕ | ⋕ |
| ENAH | enah | Protein enabled homolog | ⋕ | ⋕ |
| FLNC | flnca | Filamin-C | ⋕ | ⋕ |
| GIPC1 | gipc1 | PDZ domain-containing protein GIPC1 | | |
| GLUD1 | glud1a | Glutamate dehydrogenase 1, mitochondrial | ⋕ | |
| GNA12 | gna12a | Guanine nucleotide-binding protein subunit alpha-12 | ⋕ | † |
| GNAQ | gnaq | Guanine nucleotide-binding protein G(q) subunit alpha | † | † |
| GNB3 | gnb3a | Guanine nucleotide-binding protein G(I)/G(S)/G(T) subunit beta-3 | ⋕ | ⋕ |
| GPC4 | gpc4 | Glypican-4 | ⋕ | |
| HN1L | hn1l | Hematological and neurological expressed 1-like protein | | |
| HSD17B10 | hsd17b10 | 3-hydroxyacyl-CoA dehydrogenase type-2 | | |
| IDH3A | idh3a | Isocitrate dehydrogenase [NAD] subunit alpha, mitochondrial | | |
| INF2 | inf2 | Inverted formin-2 | | |
| KARS | kars | Lysine–tRNA ligase | ⋕ | |
| KHDRBS2 | khdrbs2 | KH domain-containing, RNA-binding, signal transduction-associated protein 2 | ⋕ | |
| LMNB2 | lmnb2 | Lamin-B2 | ⋕ | |

| Human gene symbol | Zebrafish gene symbol | Protein name | Human interaction | Zebrafish interaction |
|---|---|---|---|---|
| LRRFIP1 | lrrfip1a | Leucine-rich repeat flightless-interacting protein 1 | ‡ | |
| MAGOH | magoh | Protein mago nashi homolog | ‡ | |
| N4BP3 | n4bp1 | NEDD4-binding protein 3 | | |
| NDUFS3 | ndufs3 | NADH dehydrogenase [ubiquinone] iron–sulfur protein 3, mitochondrial | | |
| NTPCR | ntpcr | Cancer-related nucleoside-triphosphatase | | |
| P2RX4 | p2rx4a | P2X purinoceptor 4 | | |
| PABPN1 | pabpn1l | Polyadenylate-binding protein 2 | | |
| PAPSS1 | papss1 | Bifunctional 3′-phosphoadenosine 5′-phosphosulfate synthase 1 | | |
| PDK3 | pdk3a | [Pyruvate dehydrogenase [lipoamide]] kinase isozyme 3, mitochondrial | | |
| PSME3 | psme3 | Proteasome activator complex subunit 3 | † | ‡ |
| PUF60 | puf60a | Poly(U)-binding-splicing factor PUF60 | ‡ | |
| RFFL | rffl | E3 ubiquitin-protein ligase rififylin | | |
| SF1 | sf1 | Splicing factor 1 | | |
| SLC25A1 | slc25a1a | Tricarboxylate transport protein, mitochondrial | | |
| SMC4 | smc4 | Structural maintenance of chromosomes protein 4 | | |
| SMPDL3B | smpdl3b | Acid sphingomyelinase-like phosphodiesterase 3b | | |
| SMYD1 | smyd1a | SET and MYND domain-containing protein 1 | | |
| SNRPF | snrpf | Small nuclear ribonucleoprotein F | ‡ | |
| SORBS1 | sorbs1 | Sorbin and SH3 domain-containing protein 1 | ‡ | |
| SPAG1 | spag1a | Sperm-associated antigen 1 | | |
| SPTB | sptb | Spectrin beta chain, erythrocytic | ‡ | |
| SRPRB | srprb | Signal recognition particle receptor subunit beta | ‡ | |
| TMEM205 | tmem205 | Transmembrane protein 205 | | |
| TOMM70A | tomm70a | Mitochondrial import receptor subunit TOM70 | | |
| TRIM2 | trim2a | Tripartite motif-containing protein 2 | | |
| TSFM | tsfm | Elongation factor Ts, mitochondrial | ‡ | |
| TUBB2A | tubb2 | Tubulin beta-2 A chain | † | |
| VIM | vim | Vimentin | ‡ | |
| ATP4A | atp1a1a.4 | Potassium-transporting ATPase alpha chain 1 | ‡ | |
| HIST1H1D | histh1l | Histone H1.3 | ‡ | |
| PGAM4 | pgam1a | Probable phosphoglycerate mutase 4 | | |
| PLEKHG3 | plekhg3 | Pleckstrin homology domain-containing family G member 3 | ‡ | |
| RBBP7 | rbb4l | Histone-binding protein RBBP7 | † | |
| THEM6 | them6 | Protein THEM6 | | |

† Proteins sharing primary relationship with zebrafish esr1 are denoted

≠proteins sharing secondary relationships with esr1 are denoted